Work Accomplishments:

1. Tasks scheduled for Year 1

a) Decreasing horizontal grid spacing in GFDN
b) GFDN-WAVEWATCH III coupling
c) Implementation of ASIM into HWRF
d) Implementation of NCODA analysis for ocean initialization in GFDN for the Atlantic basin.

2. Tasks accomplished this period

We report here only the tasks completed since 2/01/2010. The prior tasks are reported in our semi-annual report.

Task b) GFDN-WAVEWATCH III coupling

As reported in the semi-annual report, the GFDN model has been successfully coupled with NOAA's WAVEWATCH wave model. We are in the process of conducting various sensitivity experiments to evaluate the impact of explicit wave coupling. The implemented air-sea interface module (ASIM) in the coupled system includes the following components: 1) in the hurricane model, the parameterizations of the air-sea heat and momentum fluxes and the spray source functions explicitly account for the sea state dependence and ocean currents; 2) the wave model is forced by the sea-state dependent momentum flux and will include the ocean current effects; 3) the ocean model is forced by the sea-state dependent momentum flux that accounts for the air-sea flux budget (see the coupled system diagram in our semi-annual report). The ocean current can affect the air-sea fluxes in two ways: a) by modifying the surface wave properties (wave spectra, propagation speed, etc.) and thus surface roughness, and b) by using the relative wind speed (wind speed minus current) in determining the wind stress and heat and moisture fluxes.

We have conducted a series of idealized experiments in which we explored the sensitivity of the track and intensity predictions and wind structure to the wave coupling

and the ocean current effects. In these experiments, a hurricane of Cat 3 intensity (the Hurricane Fran (1996) parameters were used to initialize the vortex) is embedded in a horizontally uniform 2.5 m/s steering wind directed eastward. The ocean was initially horizontally uniform with the initial vertical temperature profile typical for common water in the Gulf of Mexico. We present here the results of four experiments: 1 - (control) no wave coupling/no ocean current; 2 – wave coupling/no ocean current, 3- no wave coupling/ocean current, and 4 – (full coupling) wave coupling/ocean current.

Figures 1 and 2 show the sensitivity of the track and intensity (central pressure and maximum wind speed) in these four experiments. While the impact on the track is quite small, the intensity prediction (especially the maximum wind speed) is found to be very sensitive to the different coupling effects. The main reason for such sensitivity is the modulation of the drag coefficient due to the wave coupling and current effect. We show in Fig. 3 the impact of wave coupling and ocean currents on the drag coefficient separately. We found that the wave coupling can either increase or decrease the drag coefficient at high winds, depending on a specific location relative to the storm's track. The effect of ocean currents generally tends to decrease the drag in high wind conditions.
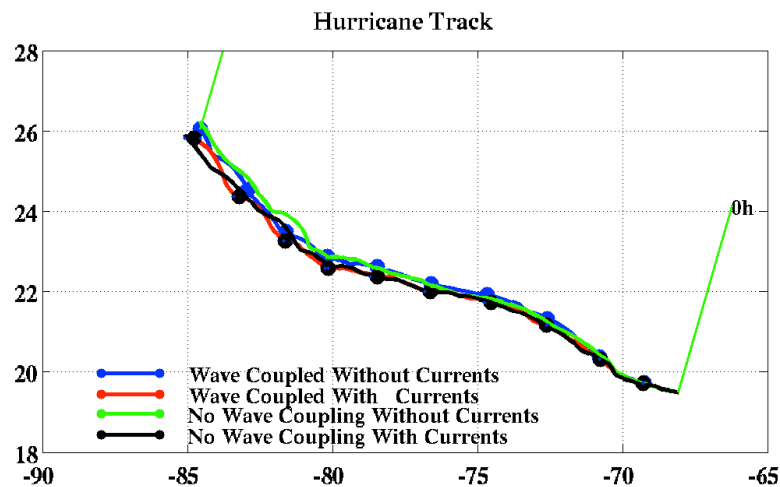

Figure 1. Hurricane tracks in four different sensitivity experiments described in the text.

Figure 4 compares spatial distributions of surface winds and drag coefficient in the control experiment and in the experiment with wave coupling and current effects after 72 hours of model integration. It is evident that the maximum drag coefficient is reduced and the maximum wind speed is increased due to wave coupling. Also, the spatial patterns are notable affected. For example, the wind speeds to the left of the track are significantly reduced in the experiment with wave coupling.

Figure 5 illustrates the impact of wave coupling and ocean currents on the spatial distribution and magnitude of the surface momentum flux. The location of maximum momentum flux has shifted from the hurricane rear in the control experiment to the right

in the experiments with wave coupling. Note that the maximum flux value is the highest when both wave coupling and current effects are included.

During the second year of this project, we will conduct a series of real-case simulations in the Atlantic basin with the new GFDL/GFDN hurricane-wave-ocean system. If the initial results show improvements in the predictive skill, we will proceed with a larger set of runs. It might be also possible to run the coupled model in a near-real time mode during the 2011 hurricane season.
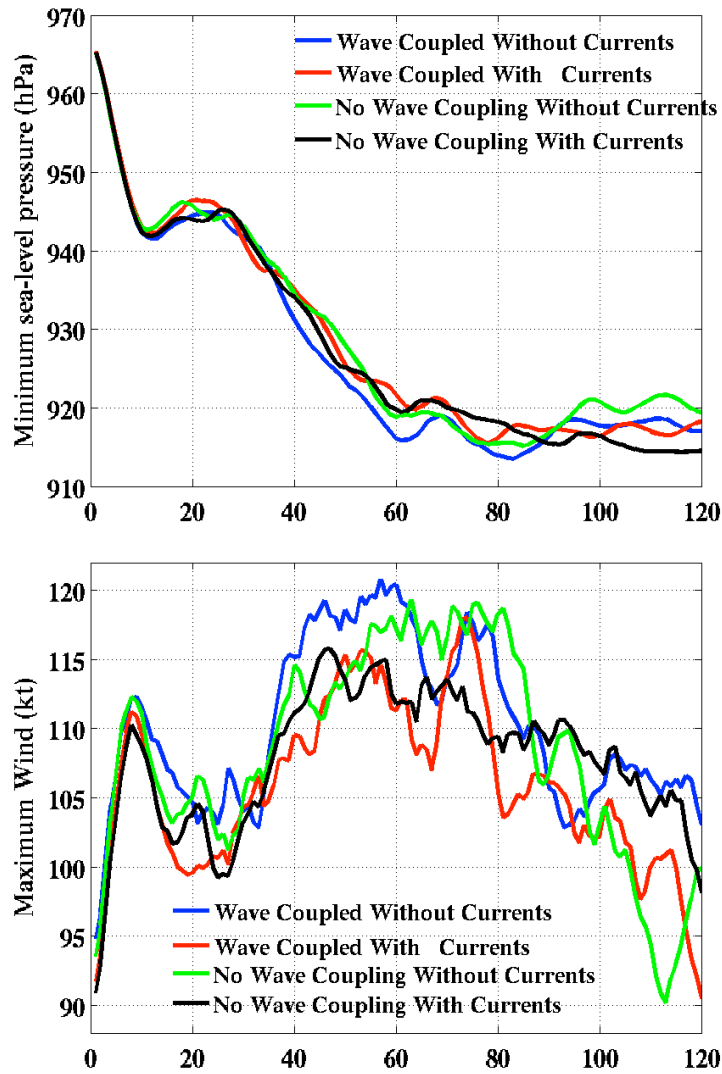

Figure 2. Central pressure (top) and maximum wind speed (bottom) in four different sensitivity experiments described in the text.
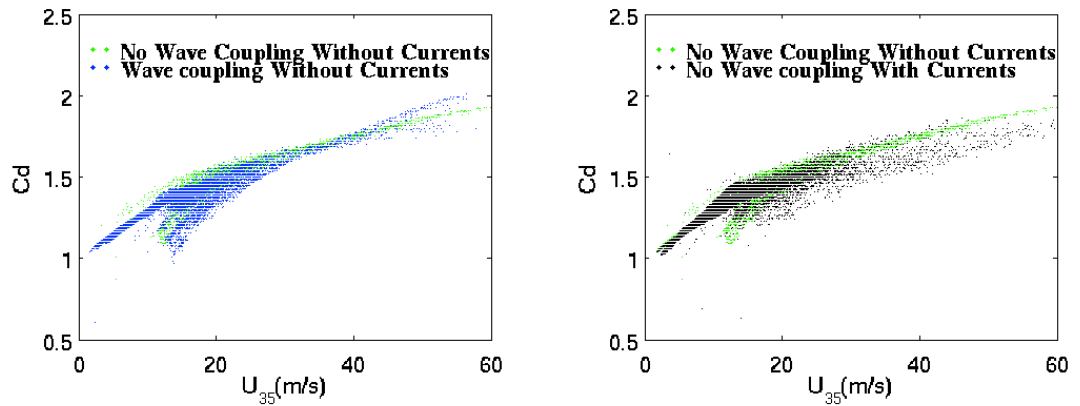
Figure 3. Drag coefficient vs. wind speed at 35 m in the coupled model experiments described in the text. Green dots are for no wave coupling/no current (control), blue dots are for wave coupling/without current, black dots are for no wave coupling/with current.
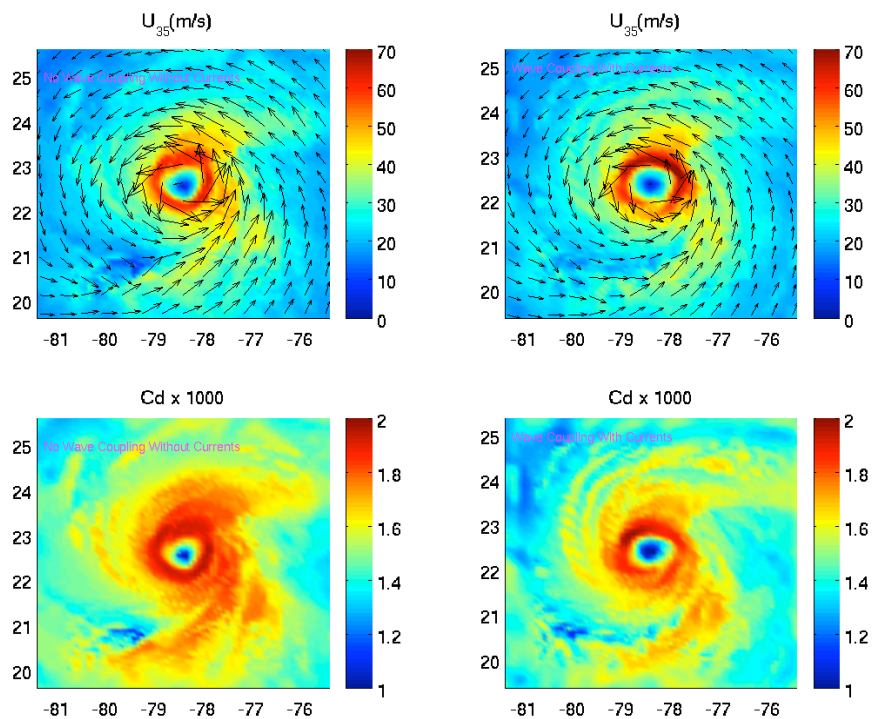

Figure 4. Wind speed at 35 m (the lowest model level) and drag coefficient in the control experiment (no wave coupling, no current effects) (top and bottom left) and with wave coupling and current effects (top and bottom right) at t=72 hr.
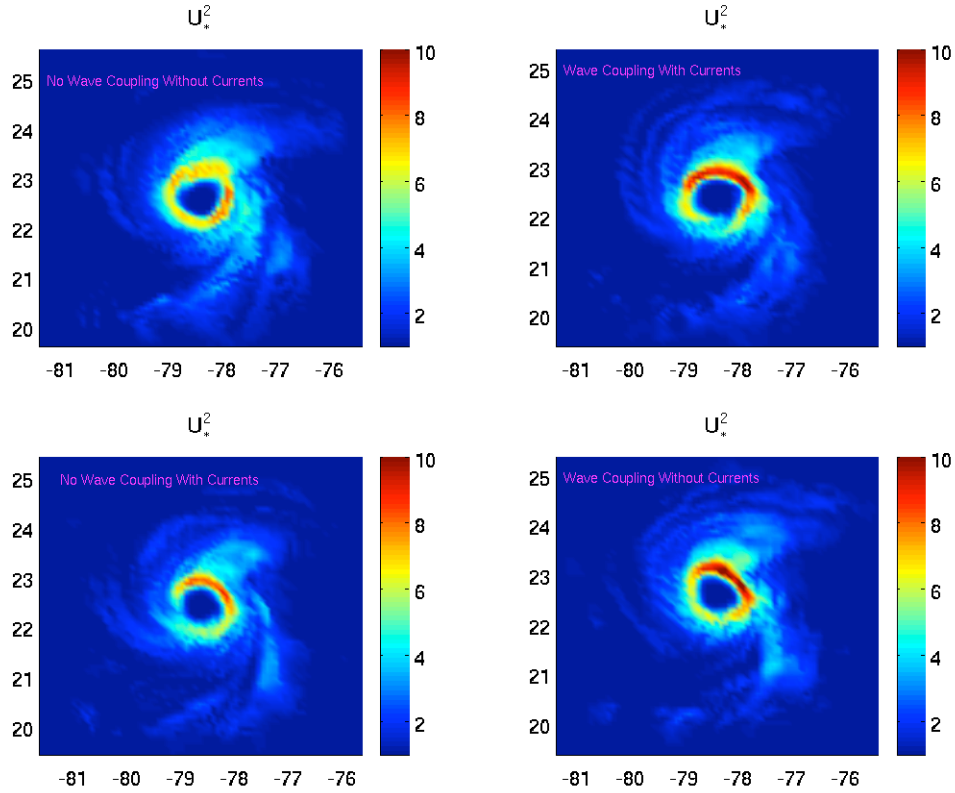
Figure 5. Normalized momentum flux (m^2/s^2) in four sensitivity experiments: a) no wave coupling without current effects (top left), no wave coupling with current effect (bottom left), with wave coupling and with current effects (top right), and with wave coupling and without currents (bottom right) at t=72 hr.

Task d) Implementation of NCODA analysis for ocean initialization in GFDN for the Atlantic basin.

We have made significant progress in the implementation of the Navy Coupled Data Assimilation (NCODA) daily temperature and salinity analysis for the Princeton Ocean Model (POM) initialization in the GFDL/GFDN coupled systems. The ocean initialization based on the assimilation of NCODA analysis may potentially replace the feature-based (F-B) initialization procedure (Yablonsky and Ginis 2008) used in the operational GFDL/GFDN models.

Here we illustrate the implementation of the NCODA analysis into the POM united domain for ocean initialization during Hurricane Ike (2008). Figure 6 shows sea surface temperature and current fields for both NCODA-based initialization and the operational F-B procedure. Although the locations of the Gulf Stream, Loop Current, and a warm-core eddy in the Gulf of Mexico are generally similar, there are notable differences in the current structures. The NCODA-based field shows some mesoscale variability, including eddies in the vicinity of the Gulf Stream that are not present in the F-B field.

Figure 7 shows temperature and velocity cross-sections across the warm-core eddy in the Gulf of Mexico. Overall, the temperature cross-sections look similar, but the temperature gradients are sharper in the F-B initialization. As a result, the maximum velocity is notably smaller in the NCODA-based initialization. We will continue evaluation of the NCODA-based initialization for other hurricane cases and assess its impact on the coupled model forecast skill during the second year of this project.
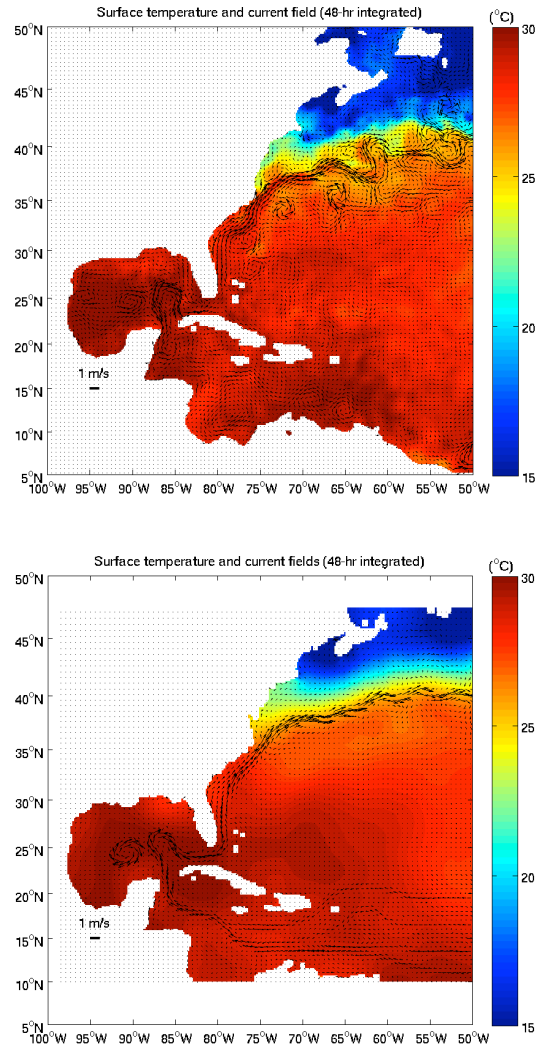

Figure. 6. Sea surface temperature and current in the POM united domain after the model initialization for Hurricane Ike (2008) using the NCODA analysis (top) and the F-B procedure (bottom).
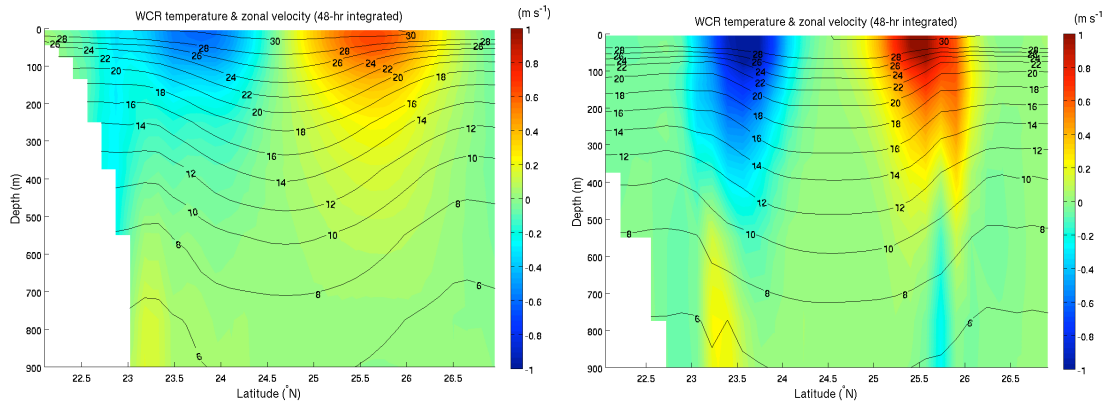
Figure 7. Temperature and velocity cross-sections across the warm core ring shown in Fig. 6.

Recently, L. Shay and G. Halliwell in their JHT Report dated 29 April 2010 expressed concerns regarding proper representation of ocean currents in the Loop Current and warm-core eddies using the F-B initialization. Our response is attached to this report as Appendix.

References:

Fan, Y., I. Ginis, and T. Hara, 2010: Momentum flux budget across air-sea interface under uniform and tropical cyclones winds. *J. Phys. Oceanogr.,* in press.

Fan, Y., I. Ginis, T. Hara, C. W. Wright, and E. Walsh, 2009a: Numerical simulations and observations of surface wave fields under an extreme tropical cyclone. *J. Phys. Oceanogr.*, 39, 2097-2116.

Fan, Y., I. Ginis, and T. Hara, 2009b: The effect of wind-wave-current interaction on air-sea momentum fluxes and ocean response in tropical cyclones. *J. Phys. Oceanogr.,* 39, 1019-1034.

Moon, I.-J., T. Hara, I. Ginis, S. E. Belcher, and H. Tolman, 2004a: Effect of surface waves on air–sea momentum exchange. Part I: Effect of mature and growing seas, *J. Atmos. Sci.*, **61**, 2321–2333.

Moon, I.-J., I. Ginis, and T. Hara, 2004b: Effect of surface waves on air–sea momentum exchange. II: Behavior of drag coefficient under tropical cyclones, *J. Atmos. Sci.*, **61**, 2334–2348.

Yablonsky, R. M. and I. Ginis, 2008: Improving the ocean initialization of coupled hurricane-ocean models using feature-based data assimilation. *Mon. Wea. Rev.,* **136,** 2592-2607.

Appendix

Response to JHT Report entitled "Problems and Recommendations Concerning the
HWRF Operational Feature-Based Ocean Initialization Procedure" by Nick Shay (RSMAS) and
George Halliwell (NOAA/AOML) dated 29 April 2010

Richard Yablonsky and Isaac Ginis (URI/GSO)
2 September 2010

Purpose: The problems in the feature-based (hereafter F-B) ocean model initialization fields produced at URI are less severe than has been reported by the Shay and Halliwell JHT Report when used correctly to spin up an ocean model prior to a coupled hurricane-ocean model forecast, as in the operational GFDL/POM and HWRF/POM systems. Therefore, in these operational systems, the vertical structure of the spun-up density and velocity fields provides an adequate initial condition for the subsequent hurricane-induced SST cooling in the vicinity of ocean features that may affect operational hurricane intensity forecasts.

Recommendation: The URI team will continue to work with G. Halliwell and the rest of the collaborative ocean model validation project team (AOML, FSU, EMC, and others) to understand the differences between the Princeton Ocean Model (POM) spin-up, which *does not* relax the density fields to the initial condition and hence allows for dynamic adjustment, and the Hybrid Coordinate Ocean model (HYCOM) spin-up, which depending on its configuration *may* relax the density fields to the initial condition (G. Halliwell, personal communication) and hence may prevent proper dynamic adjustment when used with the existing F-B model.

Background: URI provided feature-based initialization fields to G. Halliwell to be used for a POM-HYCOM comparison study (and to cross-validate idealized, POM-based, warm ocean eddy simulations performed for a manuscript in preparation), but the conclusions drawn by the Shay and Halliwell JHT report were not reviewed by URI prior to the writing or distribution of the JHT report. Herein, we first show how differences between the way POM and HYCOM adjust the F-B model density fields during prognostic ocean spin-up necessitate that results from HYCOM, as provided in the Shay and Halliwell JHT report, cannot be used to draw conclusions about the operational version of POM at NCEP/EMC. Then, we provide a review of the history and validation of the F-B model in the published literature to date. Finally, we show new work in progress towards developing and assessing an NCODA-based POM initialization as an alternative to the F-B POM initialization.

Addressing Criticism of the F-B model in the Context of Shay and Halliwell's JHT Report:
When the F-B model fields are used as the initial condition for a 48-hour prognostic integration of POM *without relaxation toward the initial condition*, as in ocean spin-up "phase 1" for the operational GFDL/POM and HWRF/POM systems, the baroclinic fronts do not slope significantly with depth. Below, Figure 1 is reproduced from the Shay and Halliwell JHT report and then an analogous SSH plot is created after a 48-hour integration of POM, initialized with the same density field from the F-B model. Notice the similarities between the two figures.
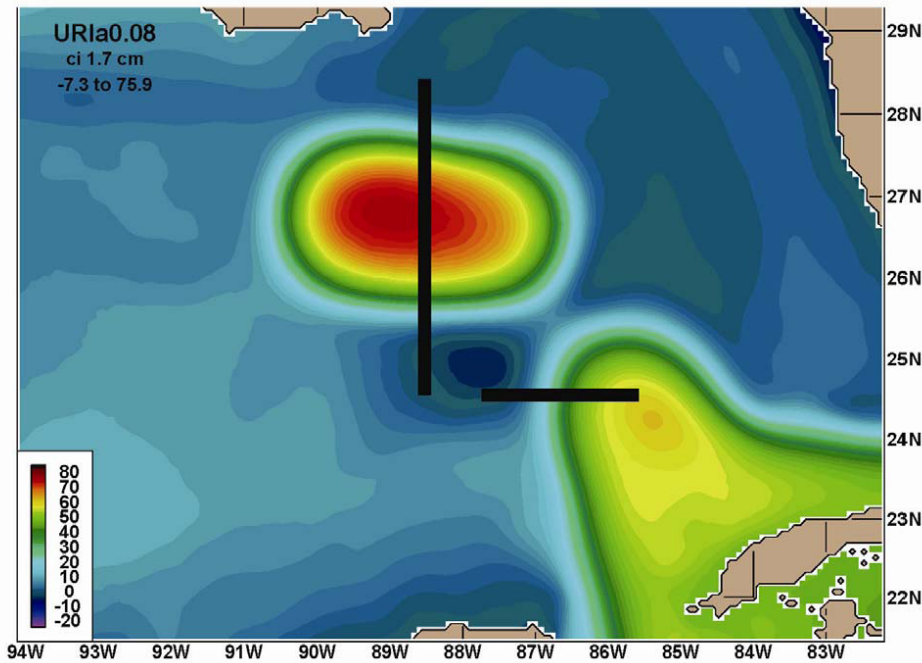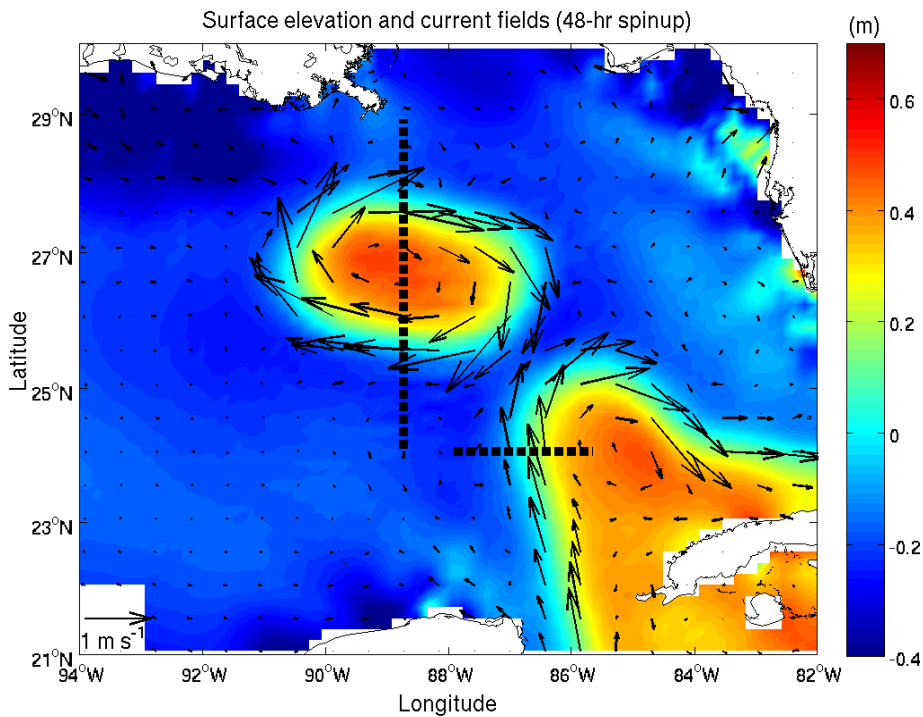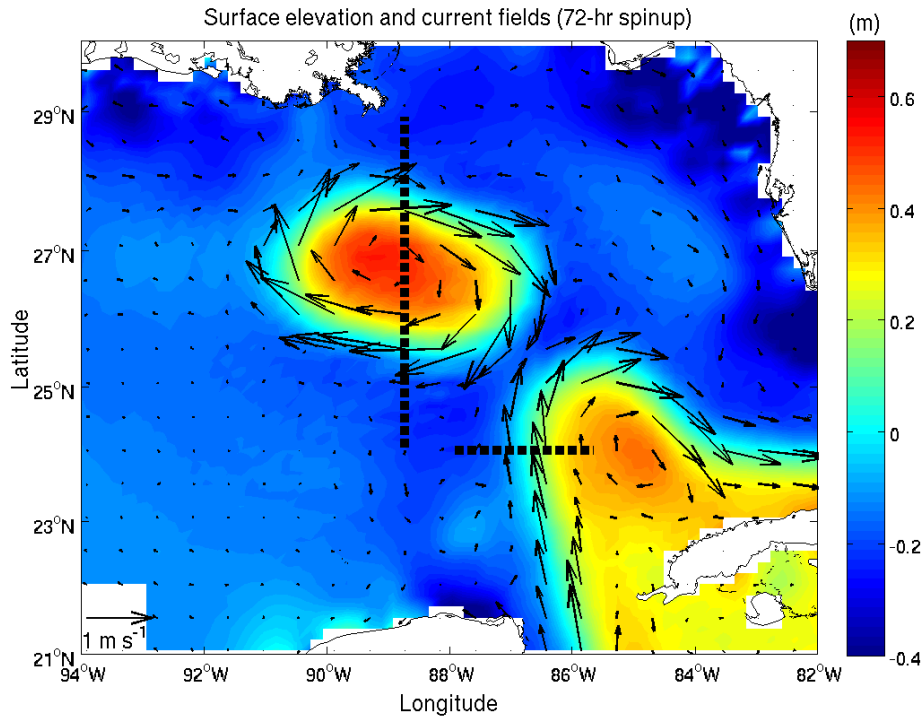
Figure 1. Pre-Ivan initial SSH map (cm) derived from the feature-based ocean model initialization product. The two cross-sections presented in Figure 2 are illustrated with black bars.

Pre-Ivan SSH map (m) and ocean currents after a 48-hour integration of POM, initialized with the F-B ocean model product.

Below, another SSH plot is created after a 72-hour integration of POM, again initialized with the same density field from the F-B model. The similarities between the 48-hour and 72-hour POM spin-ups provide evidence that the density field is in a dynamically-adjusted state by 48-hours.

Pre-Ivan SSH map (m) and ocean currents after a 72-hour integration of POM, initialized with the F-B ocean model product.

Again following the Shay and Halliwell JHT report, the subsurface structures of the Loop Current and warm core ring are investigated by examining cross sections through these features. Below, Figure 2 is reproduced from the Shay and Halliwell JHT report and then analogous velocity cross sections are created after a 48-hour integration of POM, initialized with the same density field from the F-B model. Notice that the frontal tilt in the Loop Current (especially) and the warm core ring is less pronounced in the POM simulation than in the HYCOM simulation. Also, the large vertical density jump near 650 m depth in the ring interior in the HYCOM simulation is absent from the POM simulation.
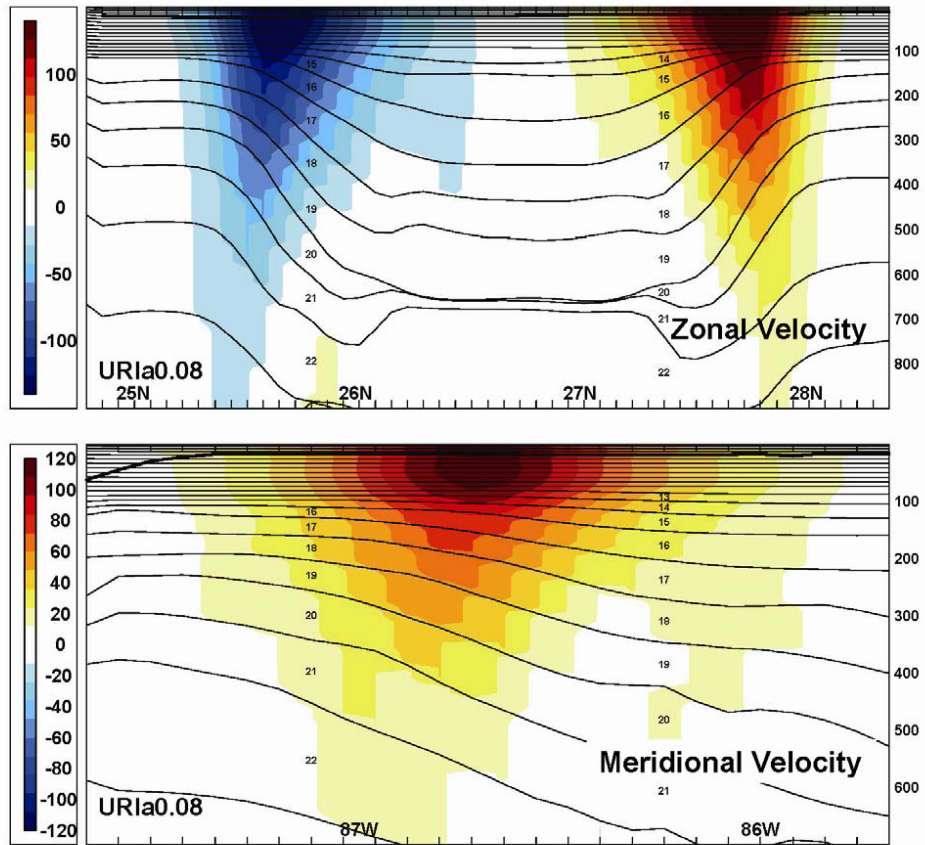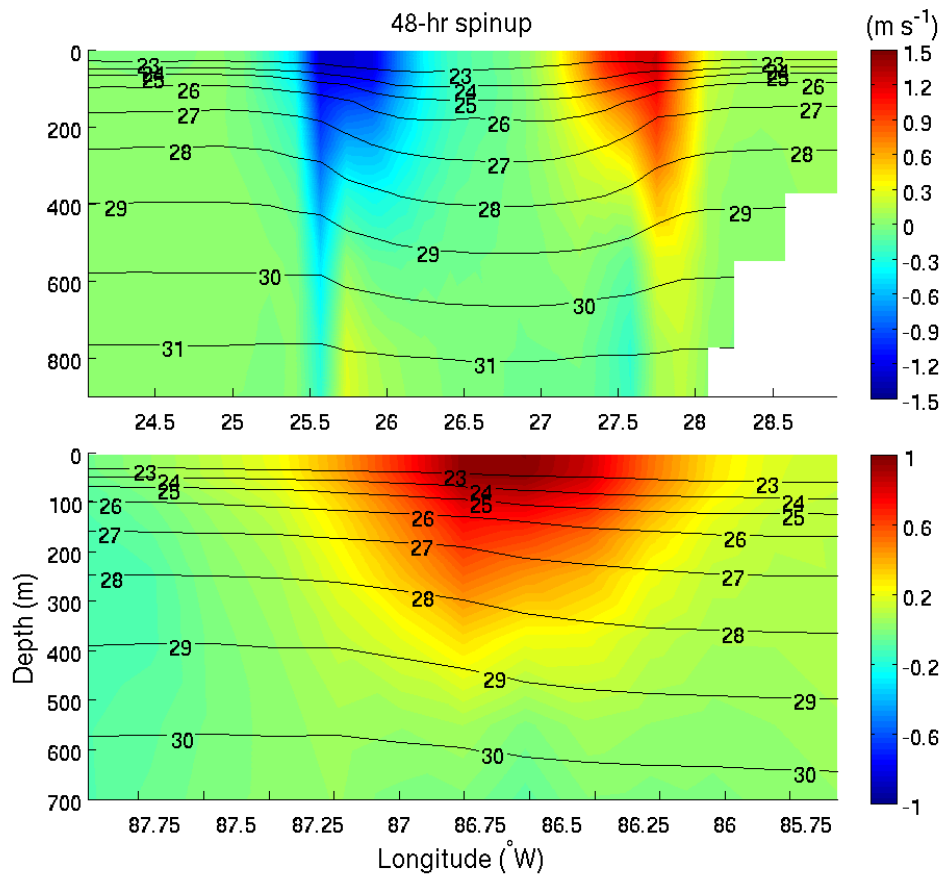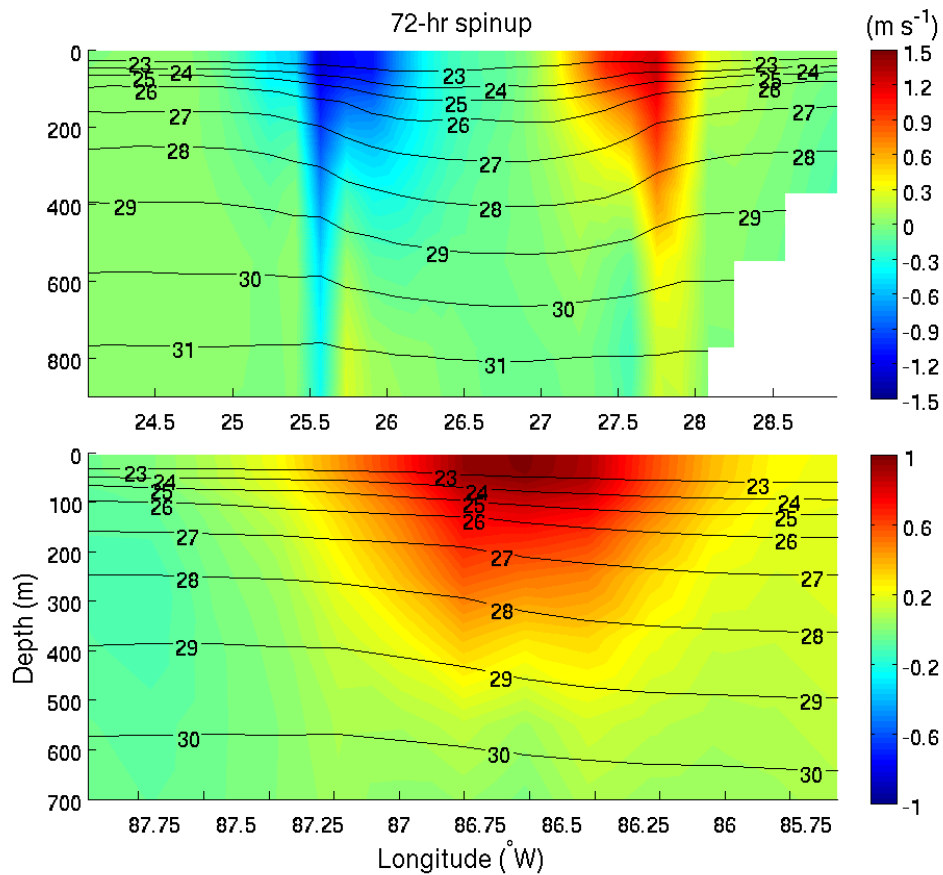
Figure 2. Pre-Ivan velocity (cm s⁻¹) cross-sections: (top) zonal velocity from a meridional section through the detached ring and (bottom) meridional velocity from a zonal section across the Loop Current. The locations of these two cross-sections are illustrated in Figure 1.
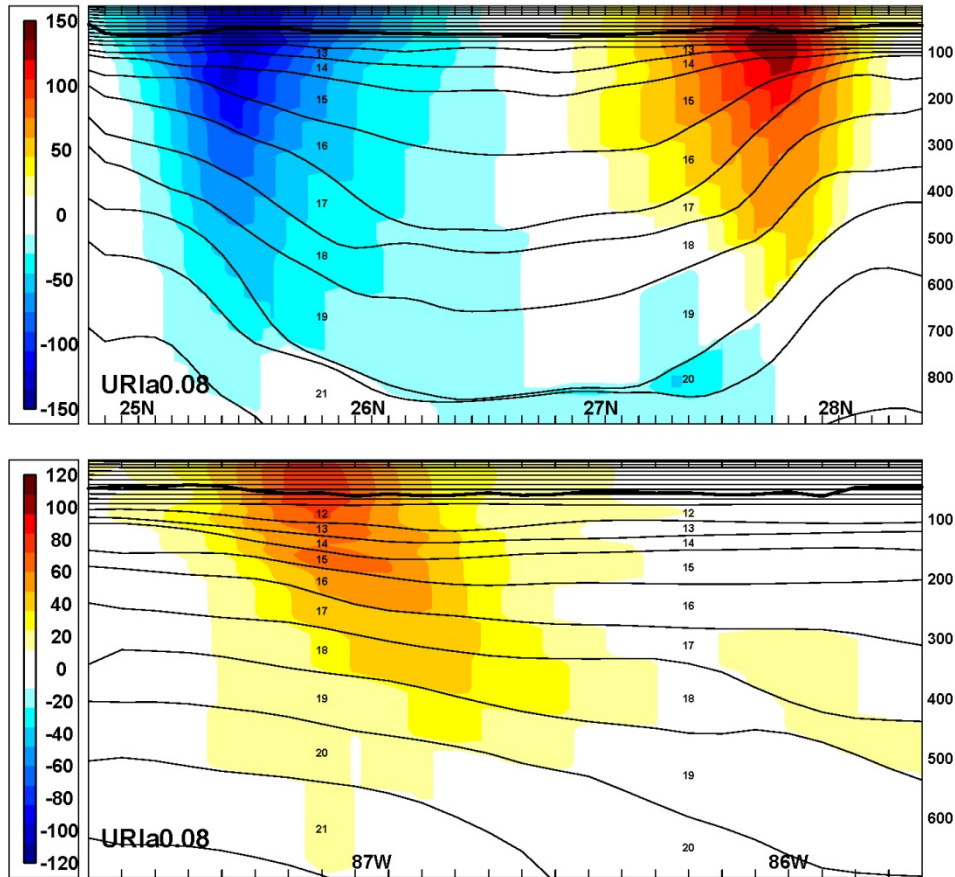
Pre-Ivan velocity (m s^{-1}) cross sections (color shaded) with density contours after a 48-hour integration of POM, initialized with the F-B ocean model product.

Below, a set of velocity cross sections is created after a 72-hour integration of POM, again initialized with the same density field from the F-B model. The similarities between the 48-hour and 72-hour POM spin-ups again provide evidence that the density field is in a dynamically-adjusted state by 48-hours.

Pre-Ivan velocity (m s^{-1}) cross sections (color shaded) with density contours after a 72-hour integration of POM, initialized with the F-B ocean model product.

After submission of the Shay and Halliwell JHT report, discussion of our concerns regarding relaxation of HYCOM to the initial T/S condition were communicated to G. Halliwell, and subsequently, G. Halliwell reran HYCOM but modified the model configuration to allow T and S to freely evolve, as in POM. The results are given below, followed by G. Halliwell's commentary on these new results.

Same "Figure 2" above from Shay and Halliwell's JHT report, but without relaxation of T and S to the initial condition.

G. Halliwell's commentary, received via email on 6 July 2010: With no relaxation, significant density adjustment did occur. For the LC, the velocity jet near the surface set up about 0.5 degrees farther west than it did when the initial ocean fields were held approximately constant. There was significant overturning associated with this adjustment that is evident in the deepening (shoaling) of model layers to the west (east) of the jet. The resulting flattening of the isopycnals produced a jet with substantially smaller maximum velocity. However, this overturning produced a baroclinic front that had a more realistic slope with increasing depth.

With T and S free to evolve, there was a similar overturning that occurred in the ring, with isopcnals deepening (shoaling) outside (inside) the ring. The resulting flattening of isopycnals around the ring boundary did reduce the maximum velocity of the current jet, but not by as much as in the LC section. However, perhaps due to the coherent structure of the ring, the correct slope of the baroclinic front did not materialize.

Some overall thoughts: When I first saw that baroclinic fronts in the initial T and S fields sloped in the wrong direction, I thought that must be a signal of a bug in setting up these fields. I realize now that this is not the case. When the ocean baroclinic fields were allowed to evolve during spinup, there was substantial correction in the initial LC frontal slope during the adjustment although there was a large decrease in maximum velocity. The ring was clearly more resistant to

change in frontal slope. Given that the remaining problems cannot be changed by a simple "bug fix" and will require significant programming, the question is whether it is feasible to undertake this significant programming.

We are moving toward using data-assimilative ocean nowcasts to initialize the ocean model, and right now, the errors and biases in these products produce more widespread SST forecast errors that the localized forecast errors that may result from problems with frontal structure present in the feature-based initial fields.

History of the F-B model: The F-B modeling approach was originally introduced by Robinson et al. (1989) and Lozano et al. (1996) and was successfully used for modeling the Gulf Stream and other oceanic fronts by Gangopadhyay et al. (1997), Robinson and Gangopadhyay (1997), and Gangopadhyay and Robinson (1997). Using ocean climatology data and the results of field experiments, they proposed analytical formulas with a set of parameters for the velocity profiles that characterize the Gulf Stream, the Deep Western Boundary Current, the southern and northern recirculation gyres, and the slope water gyre and rings. To recover temperature and salinity fields, they used a water mass model specifically developed for this part of the western North Atlantic region by Spall and Robinson (1990) and later modified by Lozano et al. (1996). The water mass model is based upon a temperature interpolation function between the Slope Water and the Sargasso Sea, and a bimodal temperature–salinity relationship. Their F-B model successfully simulated and predicted the evolution of the GS and ring detachment during the Data Assimilation and Model Evaluation Experiment (Lai et al. 1994).

The size of the so-called "united" ocean domain (i.e. Western Atlantic, Gulf of Mexico, and Caribbean Sea) in the POM component of the GFDL and HWRF coupled hurricane models is many times larger than the part of the western North Atlantic region used in the above studies. Therefore, it is difficult to convert the velocity field to temperature and salinity fields using a simple water mass model. Hence, Falkovich et al. (2005) introduced a new approach to F-B modeling in which the temperature and salinity fields are constructed to characterize the typical structure of the Gulf Stream and Loop Current by using a cross-frontal "sharpening" procedure. It is crucial to recognize that the density field that results from the Falkovich et al. (2005) F-B model is *not* meant to be completely realistic. Rather, this density field is carefully constructed such that it will adjust to a dynamically realistic (and quasi-balanced) state during subsequent prognostic integration of an ocean model *without relaxation toward the initial condition*, and during which the ocean currents are spun-up from rest. At the end of this prognostic integration, which lasts 48-hours in the operational POM (popularly referred to as ocean spinup "phase 1"), the density field is indeed in a dynamically-adjusted state, contrary to the assertions of the Shay and Halliwell JHT report. Below, we reproduce Fig. 10 from Falkovich et al. (2005), which shows how the currents in the Yucatan Channel (which become the Loop Current) are generally consistent between the F-B model (after POM integration) and observations.
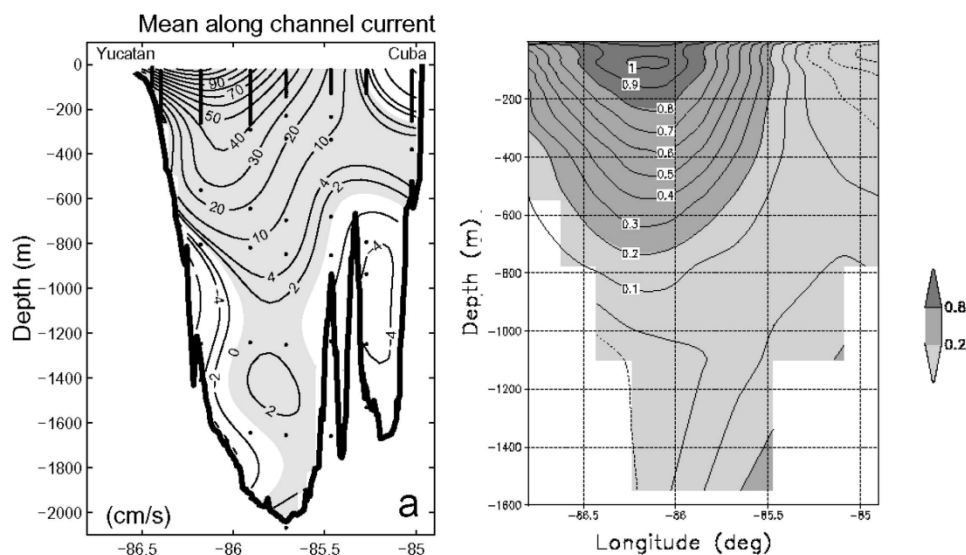
FIG. 10. Mean current along the Yucatan Channel, adopted from Sheinbaum et al. (2002). Shading indicates (left) flow into the Gulf of Mexico and (right) meridional velocity in the cross section along 21.5°N after 3 days of the coupled Hurricane Isidore forecast with the MCS initialization.

It should be noted that the observations do indicate a slight tilt in the front towards the east with depth, while the F-B model yields a front that is nearly vertical (but not severely tilted in the wrong direction, as proposed in the Shay and Halliwell JHT report). This small difference in frontal tilt between the F-B model and observations should have little impact on the storm-core SST cooling induced by a hurricane over the time scale of the hurricane; a much larger potential SST cooling impact is incorrect horizontal placement of the front, which has been an issue with many prognostic ocean models that do not either employ a F-B technique or adequately nudge their density fields towards near real-time observations.

After operational implementation at NCEP of the Falkovich et al. (2005) F-B model in the POM component of the coupled GFDL model, further improvements were made to the F-B model to create a more realistic and more flexible Loop Current shape and to include the ability to initialize warm and cold core rings in the Gulf of Mexico. These improvements are reported in Yablonsky and Ginis (2008), and comparisons are made therein among upper-ocean vertical temperature profiles from the improved F-B model (with subsequent POM phase 1 integration), a version of HYCOM available at the time, and AXBT profiles from 15 September 2005.

Below, Figs. 3 and 4 from Yablonsky and Ginis (2008) are reproduced. In Fig. 3a, the depth of the 26°C isotherm on 15 September 2005 is shown from the F-B model with subsequent POM phase 1 integration. The locations of 18 AXBT drops from that date are indicated by number. In Fig. 3b, the upper-ocean temperature profile in the center of the Loop Current is provided for two configuration of the F-B model: for the "SHA-assimilated" configuration, only satellite altimetry is used to locate the features, but for the "fully-assimilated" configuration, the feature locations and temperature profiles within the features are modified to be more consistent with the available real-time AXBTs. In Fig. 4, the upper-ocean vertical temperature profiles are compared for AXBT 1 (Fig. 4a) and 2 (Fig. 4b) from the raw GDEM climatology, the F-B model with

subsequent POM phase 1 integration (labeled as either "SHA-assimilated" or "fully-assimilated"), the aforementioned HYCOM product, and the AXBT profiles themselves.
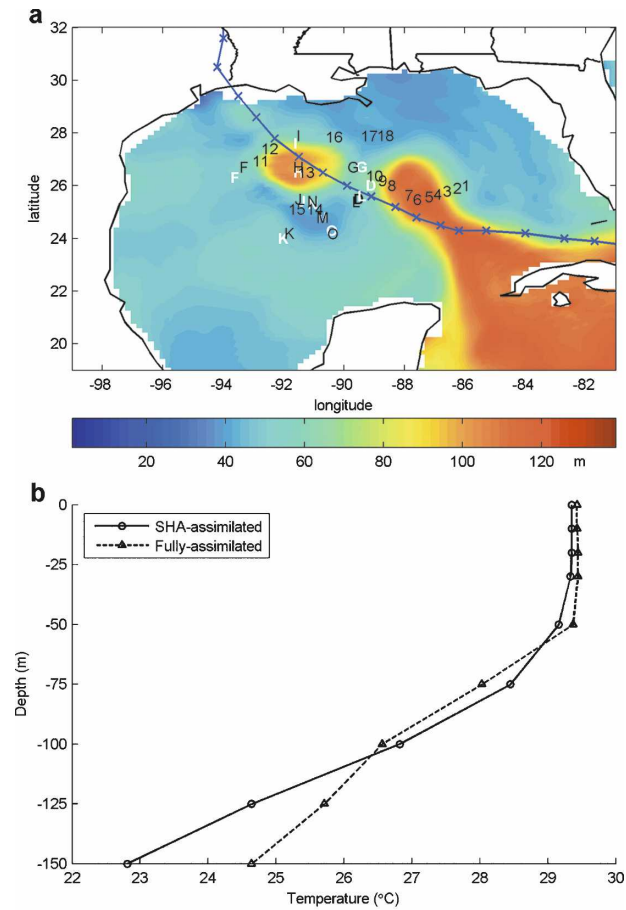

FIG. 3. (a) 15 Sep 2005 fully assimilated GoM depth of 26°C isotherm (shaded). Black letters denote LC, WCR, and CCR points that were changed for the fully assimilated case from the SHA-assimilated case (white letters). Hurricane Rita's future track is again plotted. The 18 AXBT profile locations are indicated by number. (b) SHA-assimilated (solid, circle markers) and fully assimilated (dashed, triangle markers) LCPROFILE.

FIG. 4. GDEM September climatology (dotted, "x" markers), SHA-assimilated profile (dashed, circle markers), fully assimilated profile (dashed, triangle markers), RSMAS HYCOM profile (dot-dashed, square markers), and AXBT temperature profile (solid) for (a) AXBT 1 and (b) AXBT 2. AXBT positions are given at the top of each panel; see Fig. 3a for location in the GoM basin.

Below, Figs. 5-12 from Yablonsky and Ginis (2008) are reproduced. These figures are the same as their Fig. 4 except they correspond to AXBTs 3-18.
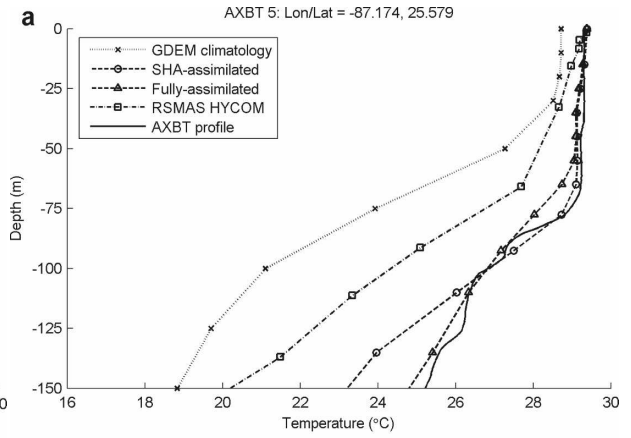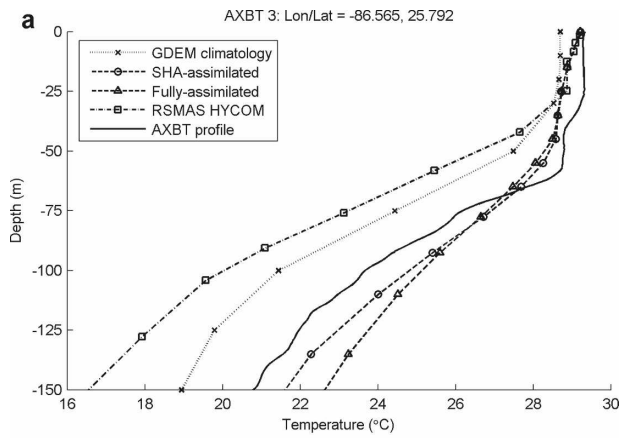
FIG. 5. Same as Fig. 4, but for AXBT (a) 3 and (b) 4.
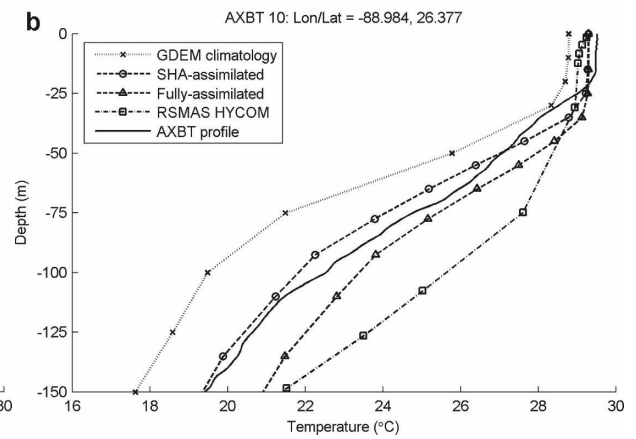
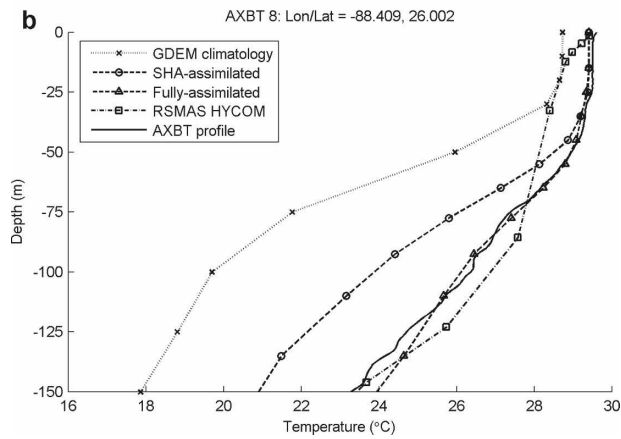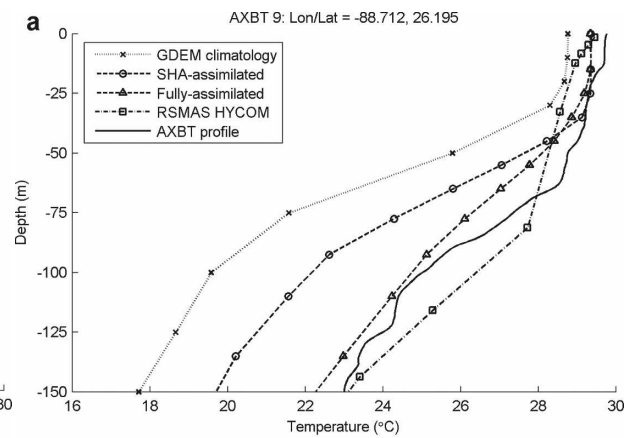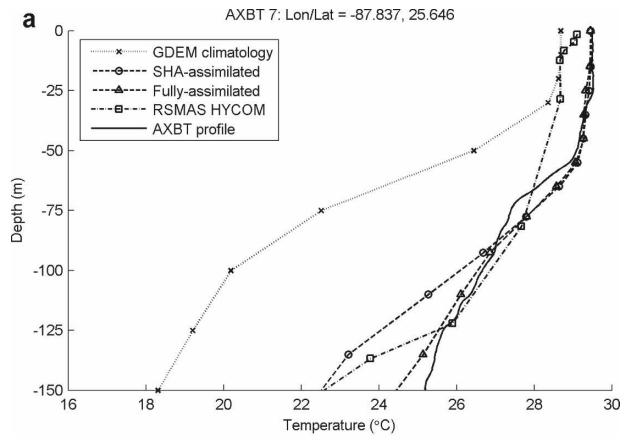FIG. 6. Same as Fig. 4, but for AXBT (a) 5 and (b) 6.

FIG. 7. Same as Fig. 4, but for AXBT (a) 7 and (b) 8.
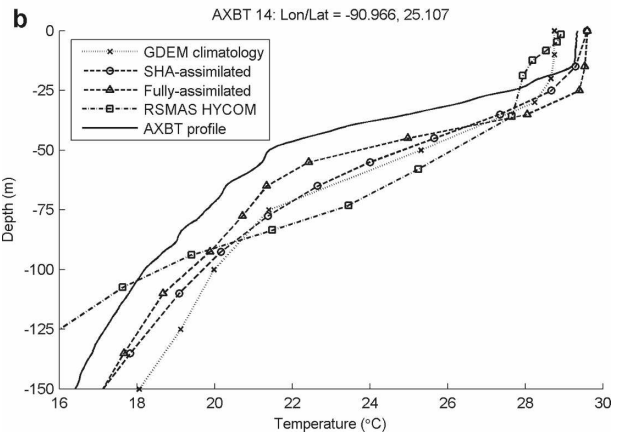
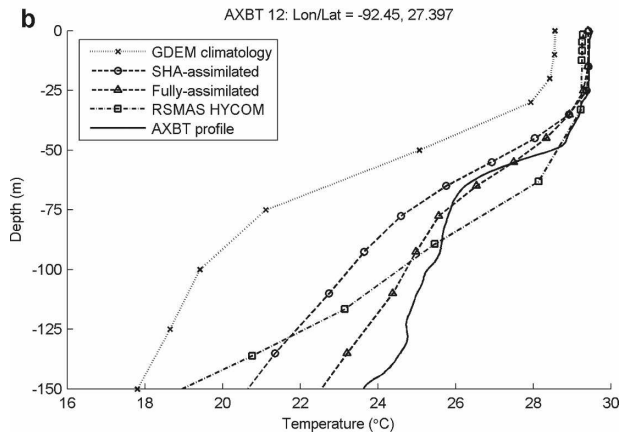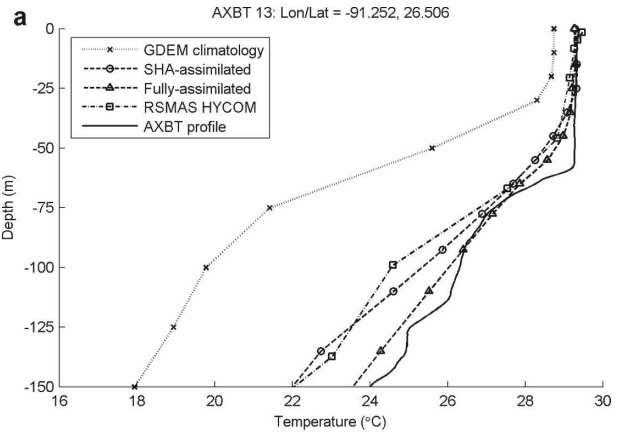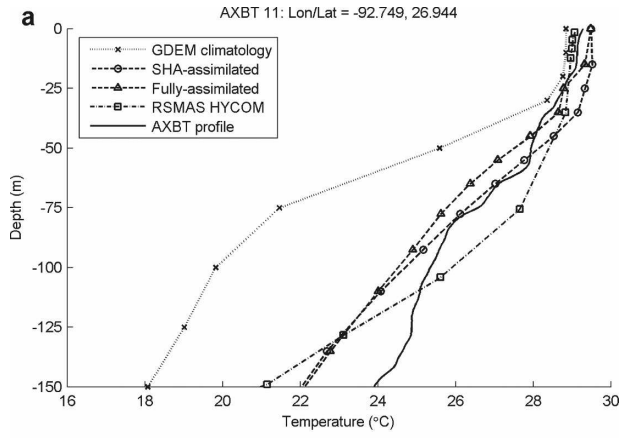FIG. 8. Same as Fig. 4, but for AXBT (a) 9 and (b) 10.

FIG. 9. Same as Fig. 4, but for AXBT (a) 11 and (b) 12.

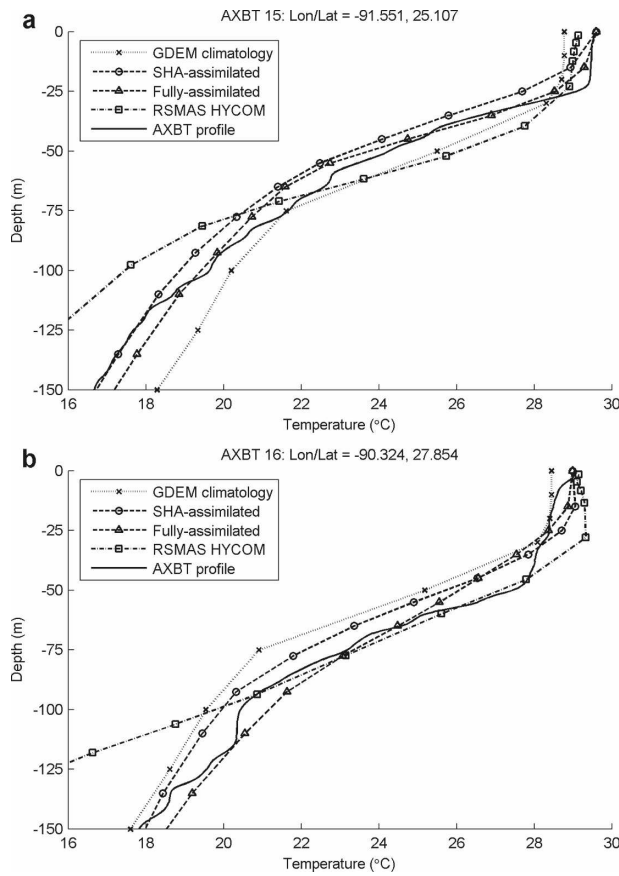FIG. 10. Same as Fig. 4, but for AXBT (a) 13 and (b) 14.

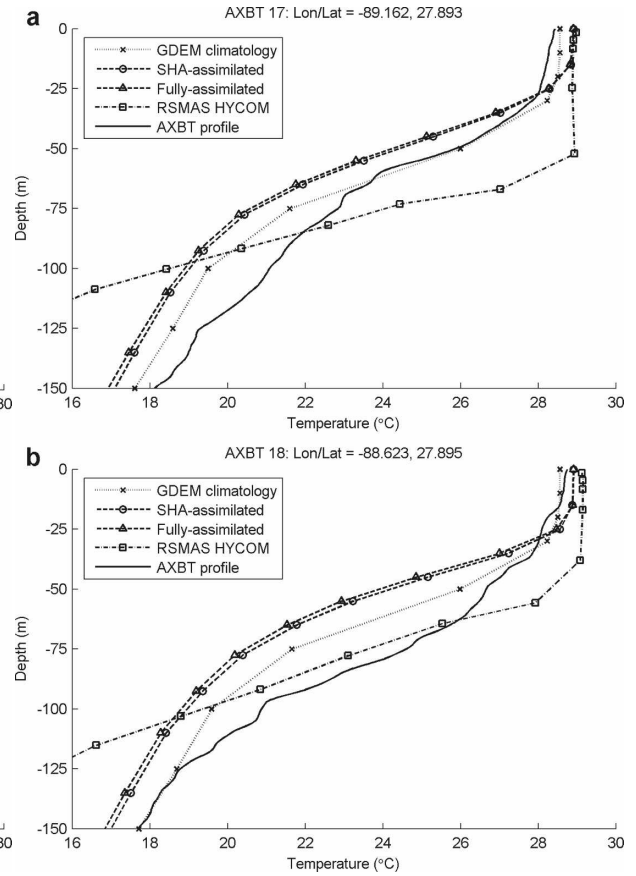FIG. 11. Same as Fig. 4, but for AXBT (a) 15 and (b) 16.

FIG. 12. Same as Fig. 4, but for AXBT (a) 17 and (b) 18.

Below, Fig. 13 from Yablonsky and Ginis (2008) is reproduced, which compares the tropical cyclone heat potential (TCHP) at the 18 AXBT locations on 15 September 2005 from the raw GDEM climatology, the F-B model with subsequent POM phase 1 integration (labeled as either "SHA-assimilated" or "fully-assimilated"), the aforementioned HYCOM product, and the AXBT profiles themselves.
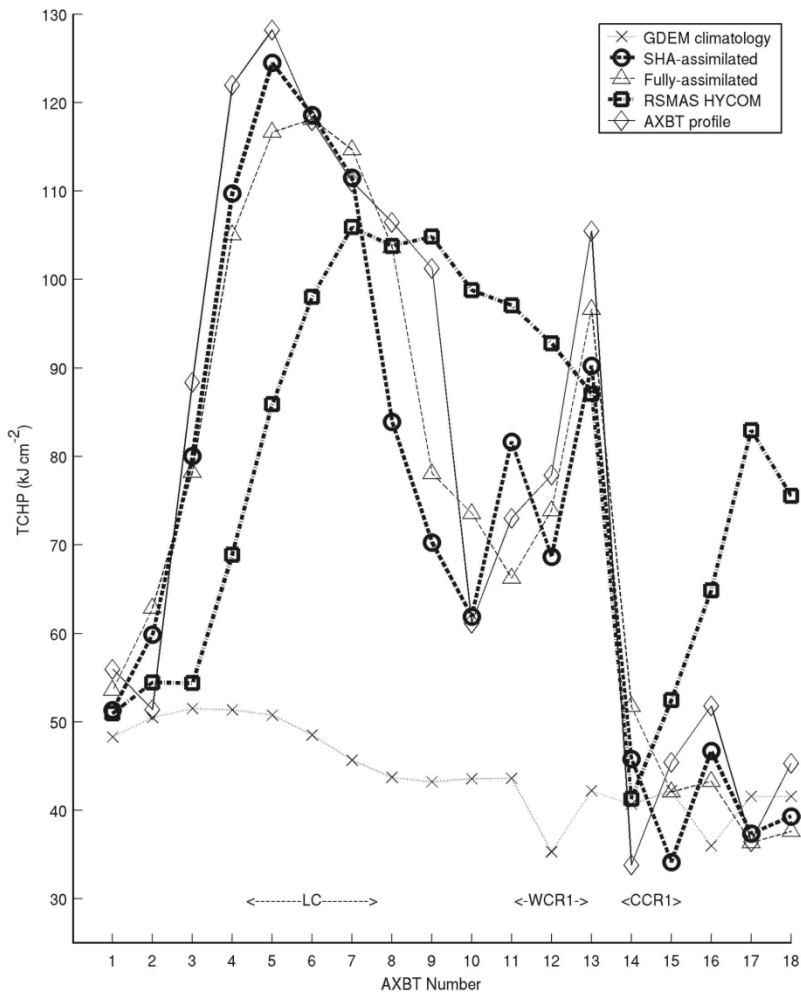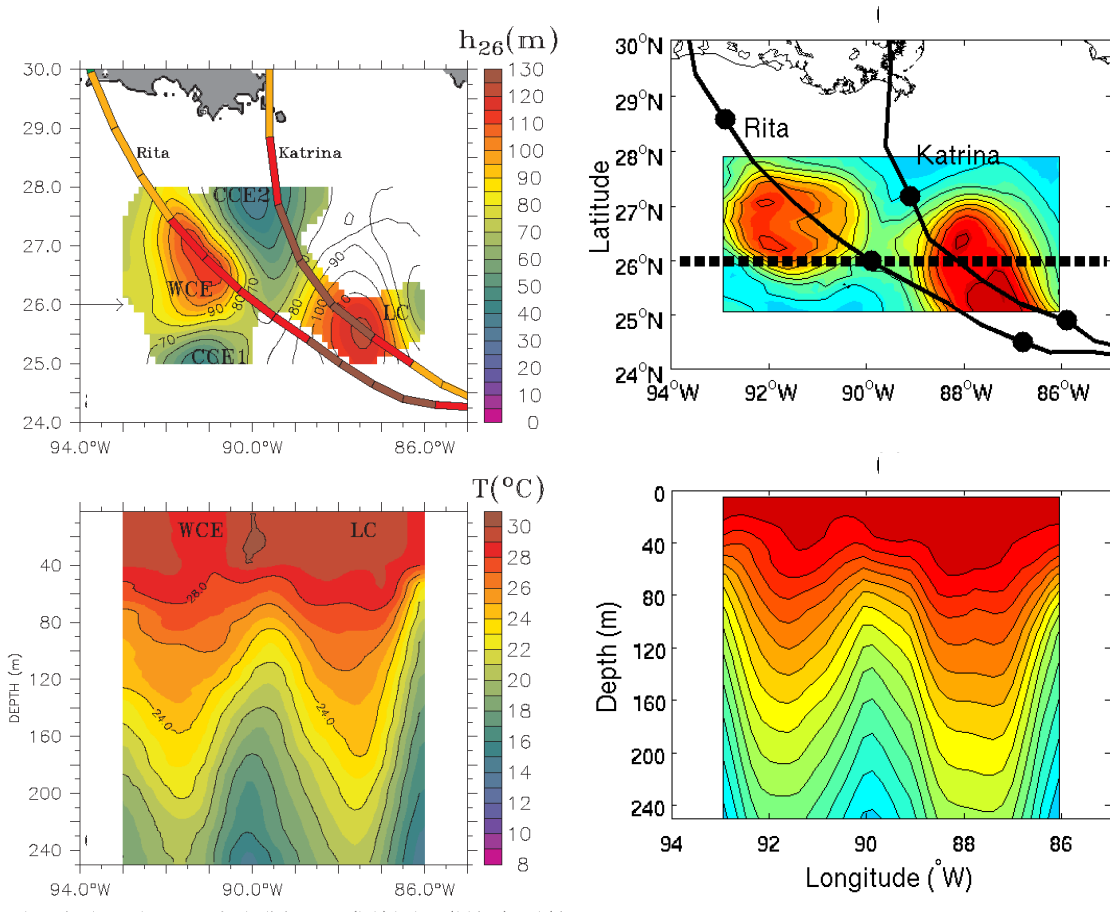
FIG. 13. TCHP at each AXBT location based on the GDEM September climatology (dotted, "x" markers), SHA-assimilated profile (bold dashed, circle markers), fully assimilated profile (dashed, triangle markers), RSMAS HYCOM profile (bold dotted–dashed, square markers), and AXBT profile (solid, diamond markers).
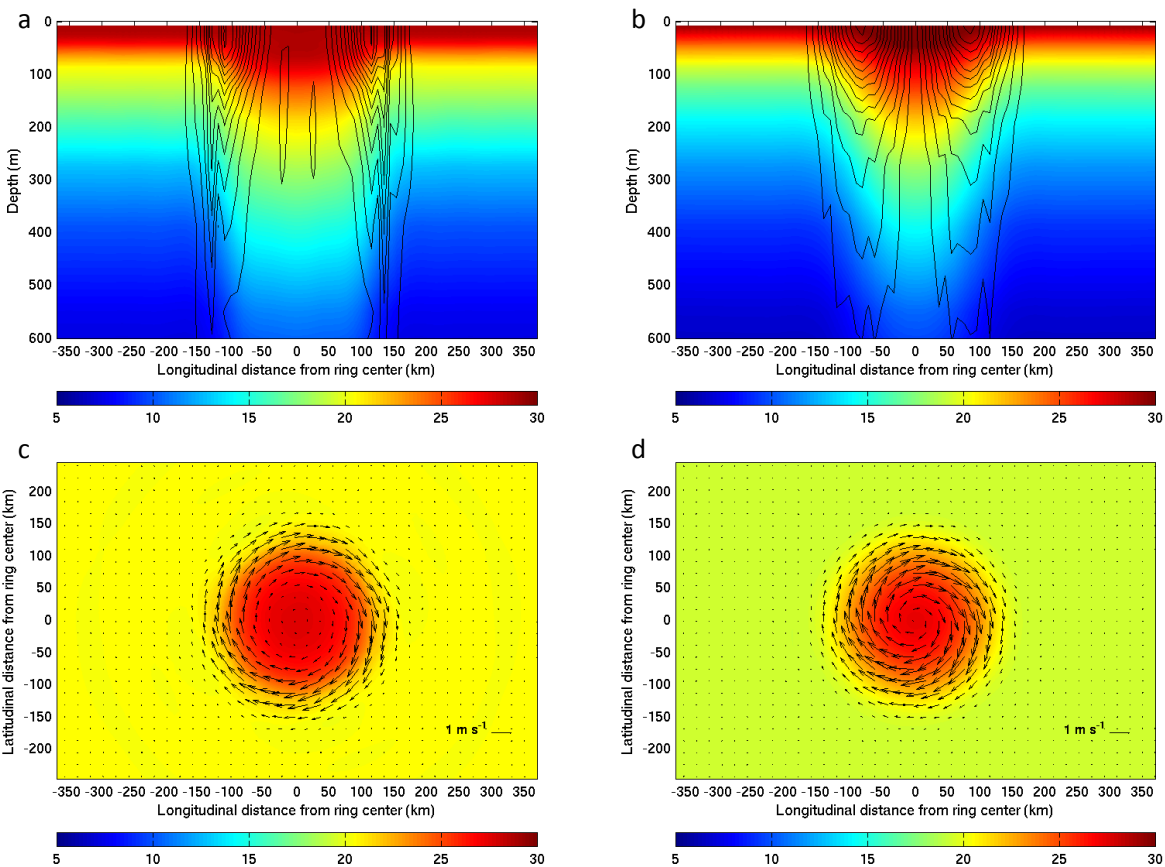
Notice that the "SHA-assimilated" and "fully-assimilated" curves are generally the most consistent with the "AXBT profile" curve.

Below is a four-panel plot that combines observationally-based Fig. 8a (upper-left) and Fig. 8c (lower-left) of Jaimes and Shay (2009) with analogous plots from POM after 48-hours of spin-up with the F-B initialization (upper-right and lower-right). The two upper panels show the depth of the 26°C isotherm, while the two lower panels show a temperature cross-section through 26°N latitude in the Gulf of Mexico. Similarities between the left panels and their respective right panels provide evidence for the F-B model's ability to reproduce the observed three-dimensional ocean temperature distribution prior to Hurricane Rita on 15 September 2005.

Thermal structure in the LC system on 15 September 2005 from airborne profilers (left), reproduced from Jaimes and Shay (2009), and from after a 48-hour integration of POM, initialized with the F-B ocean model product (right). The two upper panels show the depth of the 26°C isotherm, while the two lower panels show a temperature cross-section through 26°N latitude in the Gulf of Mexico..

Developing and assessing an NCODA-based POM initialization: Work in progress at URI includes developing an alternative POM initialization based on the NCODA analysis instead of the F-B model. Below is a comparison between an idealized, axisymmetric, F-B WCR and an idealized, axisymmetric, NCODA-based WCR. The NCODA-based WCR does not suffer from an outward-sloping current velocity field with depth like the F-B WCR does. Recall, however, that for ocean initialization of a model used to predict hurricane intensity, ocean feature *location* may often be more important than feature *structure*, so accurate placement of the features should not be sacrificed at the expense of structural improvements.

(a) POM-generated ocean temperature (°C, shaded) and current (contoured) vertical cross-section through an idealized, axisymmetric WCR, initialized using the feature-based model of Yablonsky and Ginis (2008), with the temperature and salinity profiles at the center of (outside of) the WCR defined based on the September GDEM climatology from a point in the Caribbean Sea (a point in the Gulf Common Water); (b) same as (a) but initialized by axisymmetrizing a vertical cross-section along a radius of an actual WCR in the Gulf of Mexico, as analyzed by NCODA, rather than using the feature-based model of Yablonsky and Ginis (2008); (c) ocean temperature (°C) at 87.5-m depth and current vectors at the sea surface associated with the WCR described in (a); (d) same as (c) but associated with the WCR described in (b). In both the feature-based WCR and the NCODA-based WCR, the SST has been homogenized, and any static instabilities in the initial density field have been removed by adjusting the temperature and/or salinity, as needed.

REFERENCES

Falkovich, A., I. Ginis, and S. Lord, 2005: Ocean data assimilation and initialization procedure for the Coupled GFDL/URI Hurricane Prediction System. *J. Atmos. Oceanic Technol.,* **22,** 1918–1932.

Gangopadhyay, A., and A. R. Robinson, 1997: Circulation and dynamics of the western North Atlantic. Part III: Forecasting the meanders and rings. *J. Atmos. Oceanic Technol.,* **14,** 1352–1365.

Gangopadhyay, A., A. R. Robinson, and H. G. Arango, 1997: Circulation and dynamics of the western North Atlantic. Part I: Multiscale feature models. *J. Atmos. Oceanic Technol.,* **14,** 1314–1332.

Jaimes, B., and L. K. Shay, 2009: Mixed layer cooling in mesoscale oceanic eddies during Hurricanes Katrina and Rita. *Mon. Wea. Rev.,* **137,** 4188-4207.

Lai, A., W. Qian, and S. M. Glenn, 1994: Data assimilation and model evaluation experiment datasets. *Bull. Amer. Meteor. Soc.,* **75,** 793–809.

Lozano, C. J., A. R. Robinson, H. G. Arango, A. Gangopadhyay, N. O. Sloan, P. J. Haley, and W. G. Leslie, 1996: An interdisciplinary ocean prediction system: Assimilation strategies and structured data models. *Modern Approaches to Data Assimilation in Ocean Modelling,* P. Malanotte-Rizzoli, Ed., Elsevier Oceanography Series, Elsevier Science, 413–452.

Robinson, A. R., and A. Gangopadhyay, 1997: Circulation and dynamics of the western North Atlantic. Part II: Dynamics of meanders and rings. *J. Atmos. Oceanic Technol.,* **14,** 1333–1351.

Robinson, A. R., S. M. Glen, M. A. Spall, L. J. Walstad, G. M. Gardner, and W. G. Leslie, 1989: Forecasting GS meander and rings. *Eos, Trans. Amer. Geophys. Union,* **70,** 1464–1473.

Sheinbaum, J., J. Candela, A. Badan, and J. Ochoa, 2002: Flow structure and transport in the Yucatan Channel. *Geophys. Res. Lett.,* **29,** 1040, doi:10.1029/2001GL013990.

Spall, M. A., and A. R. Robinson, 1990: Regional primitive equation studies of the Gulf Stream meander and ring formation region. *J. Phys. Oceanogr.,* **20,** 985–1016.

Yablonsky, R. M. and I. Ginis, 2008: Improving the ocean initialization of coupled hurricane-ocean models using feature-based data assimilation. *Mon. Wea. Rev.,* **136,** 2592-2607.